

# Mechanical Evaluation of Propylene Polymers under Static and Dynamic Loading Conditions

LAURA FASCE, VALERIA PETTARÍN, CELINA BERNAL, PATRICIA FRONTINI

Institute of Materials Science and Technology (INTEMA), University of Mar del Plata and National Research Council (CONICET), J.B. Justo 4302, 7600, Mar del Plata, Argentina

Received 12 November 1998; accepted 1 May 1999

**ABSTRACT:** The present investigation is concerned with the evaluation of the impact toughness of commercial-grade Propylene polymers. Conventional impact static stress-strain and static fracture experiments were carried out. Static stress-strain experiments revealed different pattern behaviors among the materials that were reflected in the fracture behavior. Under static conditions, all materials exhibited ductile behavior and crack grew under  $J$ -controlled conditions displaying stress whitening through the whole fracture surface with the sole exception of the homopolymer, which displayed a ductile instability after some stable crack growth. Under dynamic conditions the homopolymer exhibited brittle behavior, the block copolymer exhibited some plastic deformation at the crack tip, and the random copolymer samples exhibited a whitening effect due to voiding and craze formation through the whole fracture surface, indicating that stable crack propagation was occurring. Fracture mechanics tests were analyzed by following different methods, depending on the mode of fracture presented by the polymer. The Normalization  $J$ -method was used under static conditions. The elastic method, the corrected elastic method, and the essential work of fracture methodology were used to characterize brittle, semibrittle, and ductile behavior, respectively. Fracture mechanics parameters arisen from both static and dynamic conditions are compared. © 1999 John Wiley & Sons, Inc. *J Appl Polym Sci* 74: 2681–2693, 1999

**Key words:** propylene polymers; fracture modes; impact fracture parameters

## INTRODUCTION

In recent years, propylene polymers have been able to steadily increase their market share by entering new application segments. The reasons for a further continuation of this trend are a very advantageous price–property relationship and due to the fact that the homopolymer can be modified to cover a wide range of final properties. Polypropylene can be modified in different ways: during polymerization (e.g., production of syndio-

tactic homopolymers, copolymers with different comonomer content, or polymers with narrow molecular mass distribution), in the reactor (reactor blends), in compounding (e.g., manufacturing of filled and chopped fiber-reinforced grades), or in further separate processing steps (e.g., wetting of a glass mat by a PP melt, manufacturing of textile composite preforms).<sup>1</sup> The most important characteristics of these product are: molecular weight of the matrix; tacticity, crystallinity, different crystallinity forms, supermolecular structures, comonomer content, amount and type of fillers, etc.<sup>2,3</sup> The proper combination of all these properties will lead to materials exhibiting different behavior.

As in other polymeric materials, their uses are always expanding into new fields, and an ever

---

Correspondence to: P. M. Frontini.  
Contract grant sponsors: CONICET, and ANPCYT; contract grant numbers: PIP 4394/96, and 14-00000-00303.

*Journal of Applied Polymer Science*, Vol. 74, 2681–2693 (1999)  
© 1999 John Wiley & Sons, Inc. CCC 0021-8995/99/112681-13

greater performance is demanded, especially in the area of high strain rate. Because working at high speeds minimize viscoelasticity effects, and because impact is not a time-consuming technique, impact testing appears to be the most appealing practice for industry to evaluate the mechanical performance of engineering plastics. However, impact testing is one of the less understood areas of mechanical properties of polymers.

Polymer impact testing has been reviewed by different authors.<sup>4–6</sup> It is a well-known fact that impact strength is not a well-defined mechanical property. The use of a standard specimen geometry like Charpy or tensile impact<sup>6</sup> causes a severe limitation on the amount of useful information obtained on these materials. The amount of energy absorbed by the polymer during impact is dependent on many variables such as sample geometry, test temperature, impact velocity, striker shape, etc.; and relatively minor changes in any of these factors may induce the material to undergo a brittle–ductile transition. Although impact strength values give only limited information about complex high-speed failure of materials, they are one of the most widely used measures of polymer toughness. These parameters are not actual material properties, because they are strongly dependent on the specimen geometry. The Fracture Mechanics Theory provides the necessary theoretical framework to withstand the disadvantages of conventional impact testing. However, to employ this theory under impact conditions is not so simple due to dynamic effects and because it requires sophisticated acquisition data instrumentation. Over the last 20 years considerable efforts have been made to overcome the problems arising from the analysis of impact data from conventional tests using fracture mechanics specimens, and to obtain reliable stress intensity factor, energy release rate, and Integral  $J$  data on polymeric materials.<sup>6–12</sup> But despite these really valuable efforts, industry has not yet incorporated fracture analysis as a routine test.

This article reports the results of an experimental evaluation of the mechanical behavior of commercially available propylene polymers under dynamic and static conditions using both conventional and fracture mechanics kind of tests.

Three different commercial propylene polymers were assayed: one an extrusion grade homopolymer, one an impact block copolymer, and one a random copolymer. In addition, the influence of the thermal treatments that the material had undergone before testing has been taken into

account on the homopolymer. Conventional notched and unnotched Charpy tests, conventional tensile impact tests, and static tensile stress–strain deformation studies of the above-mentioned polymers were performed to assess the mechanical response.

Different behavior patterns were displayed by the materials. All the polymers displayed nonlinear behavior in static fracture experiments. Under impact conditions, however, the PP homopolymer displayed brittle fracture, the impact block copolymer displayed semiductile behavior, and the random copolymer displayed ductile behavior. Therefore, different very simple fracture mechanics approaches available in literature<sup>7,9–12</sup> and suitable for materials exhibiting linear or nonlinear behavior were tried. The Normalization  $J$ -method was used for stable fracture propagation under static conditions.  $G_{IC}$  was determined by the elastic method or elastic corrected method under impact conditions for brittle and semi-brittle behavior, respectively. The Essential Work of Fracture was used to characterize stable propagation under dynamic conditions.

## EXPERIMENTAL

### Materials and Sample Preparation

Studies were performed on different commercial grades of propylene polymers: isotactic polypropylene (PPH), 1102KX Cuyolem, generously supplied by Petroquímica Cuyo SAIC; one impact block copolymer (PPBC), 2300 PX Cuyolem, generously supplied by Petroquímica Cuyo SAIC, and one random copolymer (PPRC), Vestolen P9421, generously supplied by Dema Group SA.

Pellets were compression molded into plaques at different temperatures, depending of the polymer. The plaques of PPH and PPBC, were then annealed in an oven for 2 h at 90°C, while the plaques of PPRC were annealed for 1 h at 100°C, and then slowly cooled into the oven to room temperature to avoid the generation of residual thermal stresses. A PPH homopolymer was also annealed at 150°C (PPH-150) to promote a completely ductile crack propagation behavior.<sup>13</sup> These materials were fully characterized, and their main physical and mechanical properties are indicated in Table I. Bars for subsequent impact and fracture mechanics evaluation were cut from the compression-molded plaques and then machined to reach the final dimensions and im-

**Table I Physical and Mechanical Properties**

Material Code	Commercial Name	MFR g/10 min	$T_m$ °C	$\Delta H_m$ J/g	$\sigma_{yN}$ MPa	$\varepsilon_y$ %	$E$ GPa
PPH-150	Cuyolem 1102KX	3.4	166	100	33.7	8.7	1.46
PPH	Cuyolem 1102KX	3.4	166	97.8	31.1	10.7	1.37
PPBC	Cuyolem 2300PX	16.3	168	77.9	21.6	7.6	1.04
PPRC	Vestolen P9421	0.3	144	51.6	21.8	13.9	0.96

prove edge surface finishing. Depending on the test, 45° V or sharp notches were machined in the samples.

Dumbbell-shaped specimens for uniaxial static and dynamic testing were cut out from the 2 mm-thick molded sheets with a die.

Geometries and dimensions, specified in Figure 1(a) and (b), were chosen according to the type of testing and the equipment limitations.

### Thermal Analysis

Differential scanning calorimetry (DSC) measurements were carried out with a Du Pont 990

DSC and a Shimadzu DSC-50, at a scanning rate of 10°C/min. Standard calibrations were performed with indium and tin. The melting point was taken at the peak temperature.

### Static Measurements

Static mechanical properties were determined at room temperature, using a Shimadzu Universal S-500-C equipped with an LVDT and an extensometer and a continuous monitoring data acquisition system. Young modulus, yield strain, and yield strength were determined by stretching dumbbell-shaped specimens at a crosshead speed of 5 mm/min. Nominal yield stress was determined in the conventional way accepted for polymers as the point where the force elongation curve shows a local maximum. Static fracture experiments were carried out in three-point bending on single-edge notched specimens at 1 mm/min of a crosshead speed.

### Impact Measurements

Impact testing was carried out using a Wollpert noninstrumented Pendulum at room temperature equipped with clamps that allowed us to test samples in a tensile or three-point bending mode of loading.

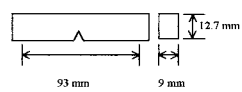
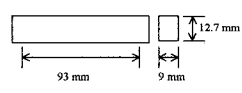
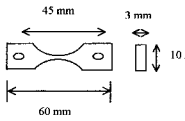
The impact fracture energy was taken directly from the scale on the machine. In the case of bending tests, the energy values reported here were corrected by kinetics effects using the following equations:

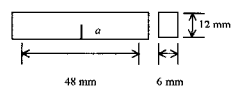
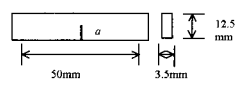
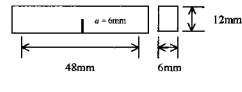
$$K_e = \frac{1}{2} m v_0^2 \quad (1)$$

$$v_0 = (2gh)^{1/2} \quad (2)$$

$$U = U' \cdot \left(1 - \frac{U'}{4 \cdot K_e}\right) \quad (3)$$

where  $g$  is the acceleration due to gravity,  $h$  is the height of fall,  $U'$  is the uncorrected energy dis-

Test Configuration	Specimen dimension	Notch Type	Test rate
Notched Charpy		V	3.5 m/s
Unnotched Charpy		None	3.5 m/s
Uniaxial Impact Tensile		None	3.5 m/s

Fracture Parameter	Specimen dimension	Notch Type	Test rate
$G_{IC}$		Sharp $0.1 < a/W < 0.9$	1 m/s
$w_c$		Sharp $0.1 < a/W < 0.8$	1.8 m/s
$J_{IC}$		Sharp	1mm/min

**Figure 1** Geometries and dimensions. (a) conventional impact experiments, (b) Fracture Mechanics experiments.

played by the instrument, and  $K_e$ , the kinetic energy of the falling mass.<sup>14</sup>

### Charpy Tests

Unnotched and V-notched specimens with dimensions according to ASTM D256 [Fig. 1(a)] were tested. Impact resistance was evaluated as the energy consumed during the impact process per unit of fractured surface area.

### Tensile Tests

Unnotched tensile impact specimens [Fig. 1(a)] were tested according to ASTM D1822-M. Impact resistance was evaluated as the energy consumed during the impact process per unit of fractured surface area.

### Fracture Mechanic Tests

Fracture mechanics determinations were carried out on precracked specimens of different thickness and a crack depth depending on the procedure adopted in each case in three-point bending at room temperature and at 1 m/s [Fig. 1(b)].

### Fracture Mechanics Data Analysis

Data points were analyzed following the different procedures proposed in the literature, depending on the type of fracture exhibited by the materials—brittle, ductile, or semibrittle—as judged from the fracture surface appearance. The validity of the model applied was double checked by the goodness of fit coming up from each model.

### Static Fracture Experiments

#### *J-R* Curve Determination

Static experiments were carried out under *J*-controlled conditions. *J-R* curves were determined by the normalization method,<sup>15–21</sup> which uses only a single precracked specimen load displacement record. *J-R* curves were constructed following the normalization routine.<sup>15</sup>

The displacement was separated into elastic and plastic components as follows:

$$v = v_{el} + v_{pl} = P \cdot C(a/W) + v_{pl} \quad (4)$$

where  $C(a/W)$  is a compliance function relating load and elastic displacement.

The deformation function was constructed by normalizing the load by the geometry function

and by assuming Power Law material type behavior.<sup>17</sup>

$$P_N = \frac{P}{G(a/W)} = \frac{P}{B \cdot W \cdot (b/W)^{\eta_{pl}}} = H(v_{pl}/W) = \beta \cdot [v_{pl}/W]^n \quad (5)$$

For the precracked record  $P_N$  can be calculated for the calibration points assuming only crack length growth due to blunting during the separable blunting zone. Then crack growth was assumed to follow the analytical expression of the blunting line

$$a_i = \frac{J}{2\sigma_0} + a_0 \quad (6)$$

For the final point  $P_N$  can be calculated, because  $a_f$  was physically determined. The deformation function can be, then, developed by regression of all these  $P_N$  calibration data points to one curve known as the key curve.

From eq. (5) we can write:

$$v_{pl} = W \cdot (P_N/\beta)^{1/n} \quad (7)$$

and from eqs. (4) and (7) and the instantaneous values of  $P$  and  $v$ , obtained from the load displacement precracked record, the instantaneous crack length can be calculated iteratively. From the instantaneous values of  $P$ ,  $v$ , and  $a$  the corresponding instantaneous values of  $J$  may be calculated to construct the *J-R* curve.<sup>17</sup>  $J_{0,2}$  was taken as the critical initiation value.<sup>22</sup>

### Dynamic Fracture Experiments

#### *Brittle Regime*

Under a completely elastic behavior, fracture occurs in an unstable manner with the aid of the strain energy stored in the sample, and the crack speed is very high in relation to that of the hammer. In this case, the critical strain energy release rate  $G_c$  can be expressed as follows:<sup>12</sup>

$$G_c = \frac{U}{C} \frac{dC}{dA} \quad (8)$$

where  $C$  is the compliance of the specimen,  $U$  is the energy absorbed by the specimen during fracture, and  $A$  is the ligament area:  $B \cdot (W-a)$ . The factor  $C/(dC/d(d(a/W))) = \phi$ , which depends on

the length of the crack size of the sample can be calculated from the following equation:<sup>23</sup>

$$\phi = \frac{\int Y^2(x)x \, dx}{Y^2(x)x} + \frac{1}{18WY^2(x)x} \quad (9)$$

$Y$  is computed from the equation given in ref. 23.

$$Y = \sum_0^4 An \left( \frac{a}{W} \right)^n \quad (10)$$

The polynomial coefficients for the span-to-width ratios ( $S/W$ ) used here were interpolated from the corresponding ones for  $S/W$  equal to 8 and 4, tabulated in ref. 24. Previous work showed that for brittle fracture behavior a basically linear relationship exists between the impact fracture energy and the specimen dimension and compliance function  $BW\phi$ .<sup>7</sup> The slope of this relationship defines the critical strain energy release rate  $G_c$  for unstable fracture.

### Semibrittle Regime

When the effects of plastic yielding are not negligible, and fracture occurs with little deformation at the crack tip, LEFM is not directly applicable because the plastic zone formed at the crack tip invalidates the model assumption. To take into account the deviations from the ideality of the model, Plati and Williams<sup>7</sup> proposed that LEFM could be extended by using an effective crack length,  $a_{\text{eff}} = a + r_p$ , where  $a$  is the original crack length, and  $r_p$  is the plastic zone length.

For this equation to be valid, the plastic zone size must be small compared to the initial crack length and the other in-plane dimensions. In the case of limited plasticity,  $r_p$  can be added to  $a$ , and then  $G_c$  can be calculated following the normal elastic procedure. We used the actual plastic zone size,  $r_p$ , which was physically measured from the fracture surface using a Profile Projector with a magnification of 20 $\times$ .

### Ductile Regime

Fracture occurs with ductile effects<sup>25</sup> such as stress whitening, surface distortion, and crack propagates in a stable mode with a continuous supply of energy from the striker to the specimen.

In this case, the fracture energy measured by an impact pendulum is a combination of crack initiation and propagation energies that include any energy to deform the material. For such a case through this article, the Essential work of fracture was chosen as a ductile fracture methodology. From a practical point of view, this method appears easier to apply than the commonly used  $J$ - $R$  curve determinations under impact conditions,<sup>9,26</sup> because it avoids stopping the test to measure the crack growth.<sup>27,28</sup>

The Essential work of fracture was first applied for the evaluation of low-rate fracture toughness of very ductile polymers in plane stress,<sup>29-33</sup> but can also be applied for the evaluation of polymer toughness at high-rate and in-plane strain conditions.<sup>9,25,34-36</sup> The work of fracture is partitioned into two parts. One is the work into the end region in the vicinity of the crack tip, which initiates the crack, and represents the energy dissipated in the fracture process zone, where necking and fracture occur. The other is the work into the outer region that is responsible for plastic deformation. Under plane stress conditions the total specific fracture work,  $w_f$ , may be defined as

$$w_f = w_e + l \cdot \beta \cdot w_p \quad (11)$$

where  $w_e$  is the specific essential work of fracture, which is a material constant for a given sheet thickness, and may be a useful material constant for characterizing the fracture toughness of ductile materials. It is defined as essential work in the specimen width per unit thickness,  $B$ , and unit ligament length,  $l$ .  $w_p$  is the nonessential work of fracture dissipated per unit volume of the material, and is not a material property because its value depends on the specimen and crack geometry.  $\beta$  is a shape factor for the outer plastic zone.

Under plane stress conditions, the plot of the specific work of fracture,  $w_f$ , as a function of ligament length,  $l$ , should yield a straight line. Inherent in this equation is the assumption that the size of the plastic zone is controlled by the ligament length.

It has been shown that for  $l < 3B$ , a plane stress-plane strain transition occurs.<sup>9,37-39</sup> In such a situation, when the ligament length-to-thickness ratio goes to zero, the fracture goes to plane strain,  $w_f$  decreases to the value  $w_{Ie}$ , provided that the specimen thickness,  $B$ , satisfies the plane strain condition:

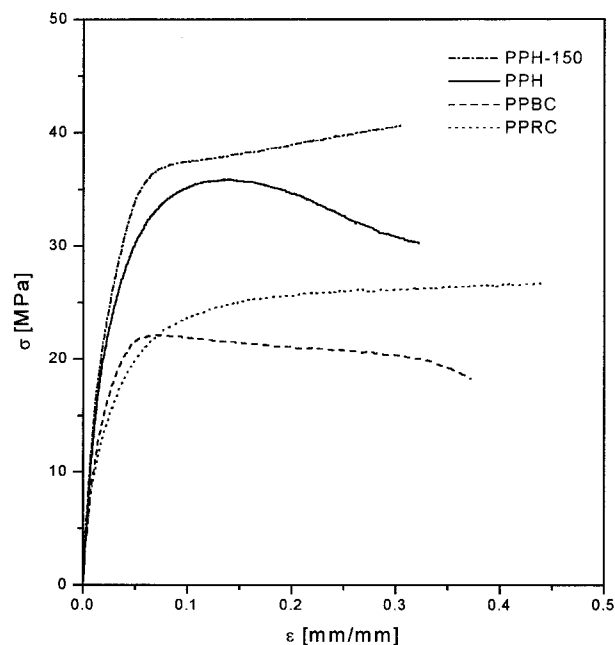


**Figure 2** True stress vs. strain curves for the different polypropylene polymers.

$$B > 25 \cdot w_{Ie} / \sigma_y \quad (12)$$

where  $\sigma_y$  is the yield stress of the material, and  $w_{Ie}$  is the plane strain specific essential work of fracture.

## RESULTS AND DISCUSSION

### Thermal Properties

Thermal properties are specified in Table I. The thermal treatment applied to the homopolymer (3 h at 150°C) induced a slight increase in the DSC-measured heat of fusion for the homopolymer, which can be taken as a measure of crystallinity. As expected, the lowest value of the specific heat of fusion was exhibited by the random copolymer and the intermediate value by the block copolymer. Melting temperature (which could be taken as an indication of the lamella thickness) was practically different only for the random copolymer, which was sensibly lower. Before the main peak a polypropylene block like PPBC displayed a shoulder that can be interpreted as the fusion of the copolymer, while the main peak corresponds to the fusion of the polypropylene block.

### Static Uniaxial Stress–Strain Behavior

The deformation behavior and ultimate mechanical properties are very important characteristics

of semicrystalline polymers. These macroscopic properties are known to very closely depend on the molecular structure and the level of crystallinity, so their knowledge is considered essential. The mechanical properties arising from the analysis of the stress–strain curves are shown in Table I and in Figure 2, respectively. Polymers were ordered in decreasing trend with Young's modulus in conjunction with the trends in the specific heat of the fusion displayed by the materials. Thermal treatment slightly increased  $\sigma_y$ , and the Young's modulus of the homopolymer consistent with the higher crystallinity values displayed by PPH-150 samples.

Typical uniaxial sample specimens, after being deformed, are shown in the photograph of Figure 3. All the polymers showed stress whitening while deformed, but a cursory examination of the stress–strain curves shows that each polymer followed a different pattern, with noticeable differences.

The homopolymer (PPH) and the annealed homopolymer (PPH-150) samples formed a very marked neck with localized stress whitening; the remainder of the gauge length was not plastically deformed. After reaching the maximum, the stress drop without strain hardening and the sample thinned to failure, displaying a flow-induced failure caused by the inability of the neck to stabilize.

The block copolymer (PPBC) displayed an intermediate behavior between the homopolymer and the random copolymer. It showed a less defined stress maximum, and beyond the maximum the sample extends uniformly up to the fracture with diffused stress whitening and without neck-

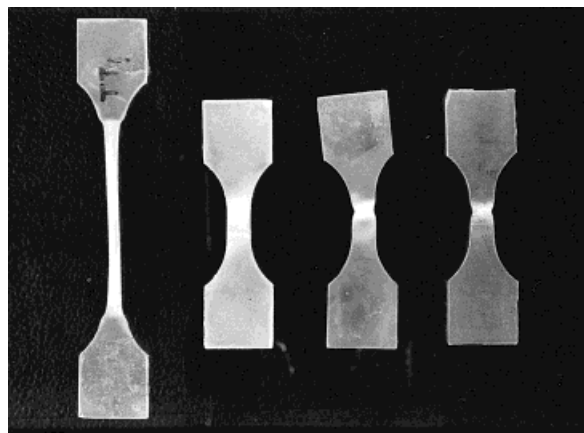


**Figure 3** Typical uniaxial tensile specimens deformed after yielding under static loading conditions.

**Table II Conventional Impact and Fracture Mechanics Testing Results**

Material	Conventional Impact Strength			Fracture Mechanics Parameter	
	Notched Charpy $J/mm^2$	Unnotched Charpy $J/mm^2$	Tensile Impact $J/mm^2$	Dynamic Loading N/mm	Static Loading N/mm
PPH	0.003	0.007	0.082	$G_{IC}=2.5$	$J_{02}=15.6$
PPH-150	0.005	0.016	0.097	$G_{IC}=2.4$	$J_{02}=13.8$
PPBC	0.006	0.060	0.112	$G_{IC}=6.8$	$J_{02}=8.1$
PPRC	0.019	N-B	0.166	$w_e=8.3$	$J_{02}=9.7$

ing. The slight drop in  $\sigma_y$  was not enough to support the formation of a stable neck and drawing.

The PPRC sample formed a very marked stable neck that which extended throughout the whole test piece steadily to the point of fracture at a very large deformation value. Samples showed a sharp stress maximum (upper yield point), after which the stress dropped to the lower yield stress. Beyond this point there was a decrease in load with a further increase in elongation; the force then remained essentially constant, with a further increase in length, and due to strain hardening, the necked extended uniformly.

### Conventional Impact Testing

The results of conventional impact testing are summarized in Table II. The three tests gave the same material ranking but the differences in toughness among them depended on the test performed. The toughest material was the random copolymer, followed by the block copolymer, the annealed homopolymer, and the untreated homopolymer.

None of the homopolymers showed signs of stress whitening in any of the Charpy tests, even if thermal treatment improve the homopolymer performance (Table II). The PPBC notched specimens were all found to fracture in the impact tests with some microscopic deformation; nevertheless, the size of the plastic zone was reduced by the presence of the notch. PPRC showed a large degree of stress whitening in any case.

Testing of both unnotched<sup>40</sup> and notched specimens allows us to understand the important problem of polymer notch sensitivity. If unnotched, the measured impact strength is influenced by the energy required for both crack initiation and subsequent propagation. But if the specimen contains a sharp notch, then the stress places a greater emphasis on the material resistance to crack propagation toughness. In every

case, the unnotched impact energy was always higher, indicating the important contribution of the initiation process to impact strength. This effect was especially visible in the block copolymer and the random copolymer. The former exhibited extremely higher unnotched Charpy energy values, while the latter did not even break at all.

The tensile impact test has the same physical meaning as the quasistatic uniaxial tensile test by measuring tensile property at a high strain rate.<sup>6</sup> Samples of block copolymers and random copolymers displayed stress whitening all over the gauge length, while both homopolymers broke in a brittle manner. Tensile energy values were higher than Charpy values, probably due to the smaller constraint of this test; nevertheless, no large differences in the specific energies among the propylene polymers were found. This test appears to be a very fair selective in characterizing this kind of materials.

As previously stated,<sup>6</sup> the results obtained by these kinds of tests are difficult to compare because the stress distribution is different, so that it is impossible to unify the results; in fact, no simple correlation between them was possible to obtain.

### Fractographic Analysis and Fracture Modes

#### Static Fracture Experiments

Under static conditions all materials exhibited nonlinear load-line displacement traces coming up from the growth of a significant damage zone at the crack tip ("stress whitening") as well as from the initiation of subcritical growth before the maximum load was reached (Fig. 4). Photographs of fracture surface features are shown in Figure 5. Under such a situation LEFM hypothesis are invalid, so that Integral- $J$  was selected as a fracture criterion. PPH-150, PPBC, and PPRC samples

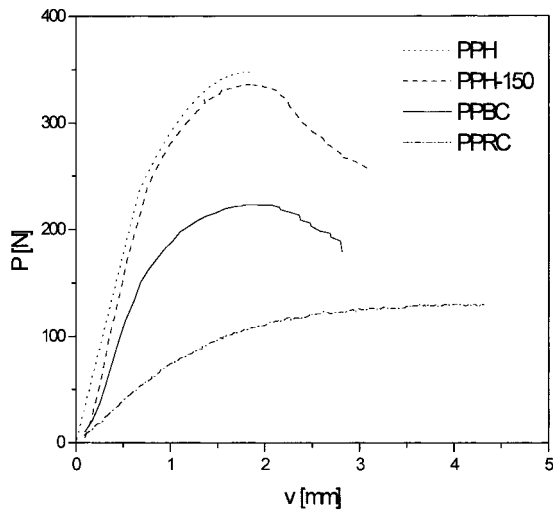


**Figure 4** Load vs. displacement plots for the different propylene polymers (static fracture experiments).

displayed a completely stable fracture: the crack grew with the continuous supply of energy from the external load and with continuous increase in displacement until complete fracture. Only the PPH samples exhibited a different pattern: at a certain deflection level after the maximum load, after a certain amount of stable propagation had occurred, sudden instability occurred (Fig. 4), and the specimen broke in two halves, which literally flew away, aided by the energy provided by the elastic strain energy stored in the sample.<sup>41–43</sup> Fracture surface inspection [Fig. 5(a)] allows us to appreciate the instability point. So, the  $J$ - $R$  curve was determined only during the stable stage where the  $J$ -controlled condition is valid.

#### Dynamic Fracture Experiments

Under dynamic conditions the presence of brittle or ductile fracture was judged from the appear-

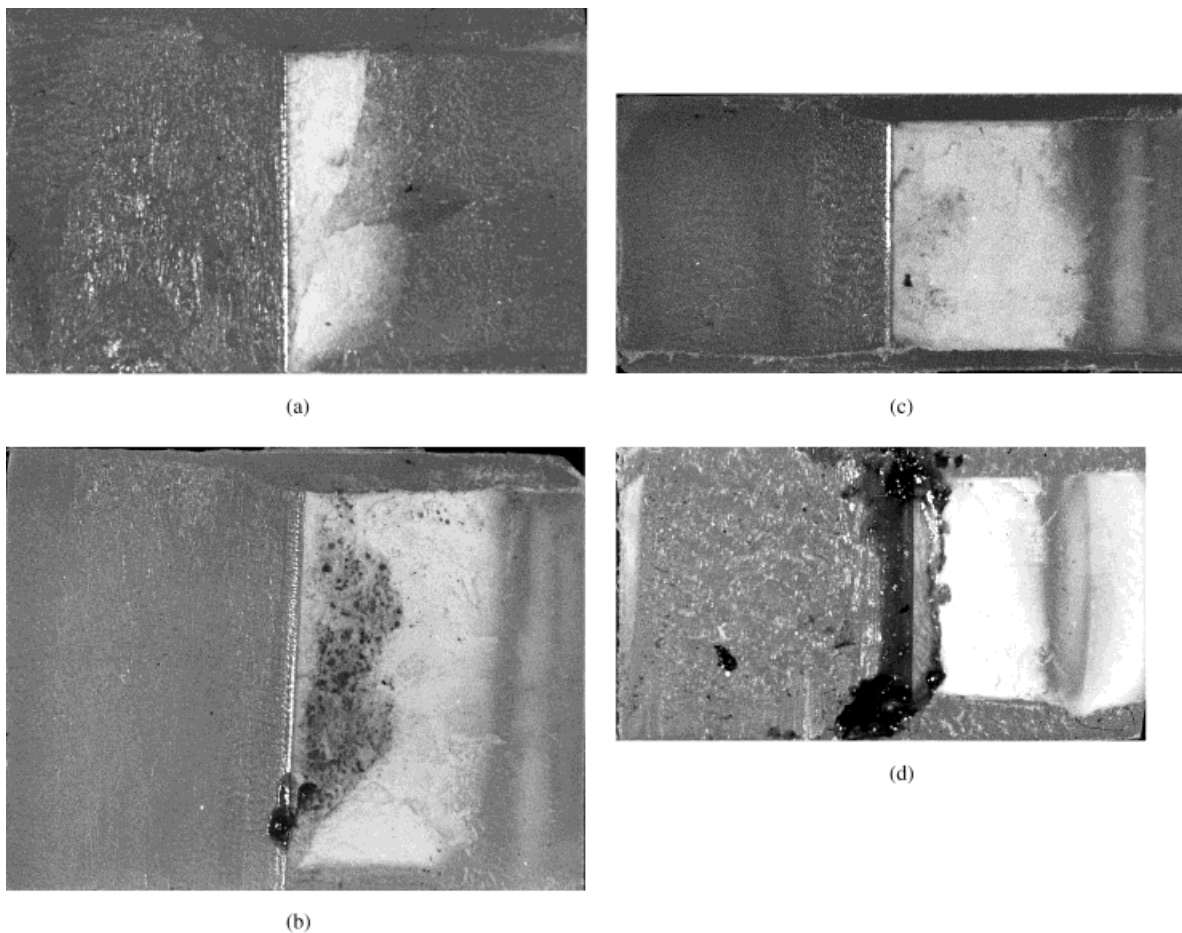


**Figure 5** Fracture surface of propylene samples broken under static loading conditions (direction of propagation from left to right). (a) PPH, (b) PPH-150, (c) PPBC, (d) PPRC.



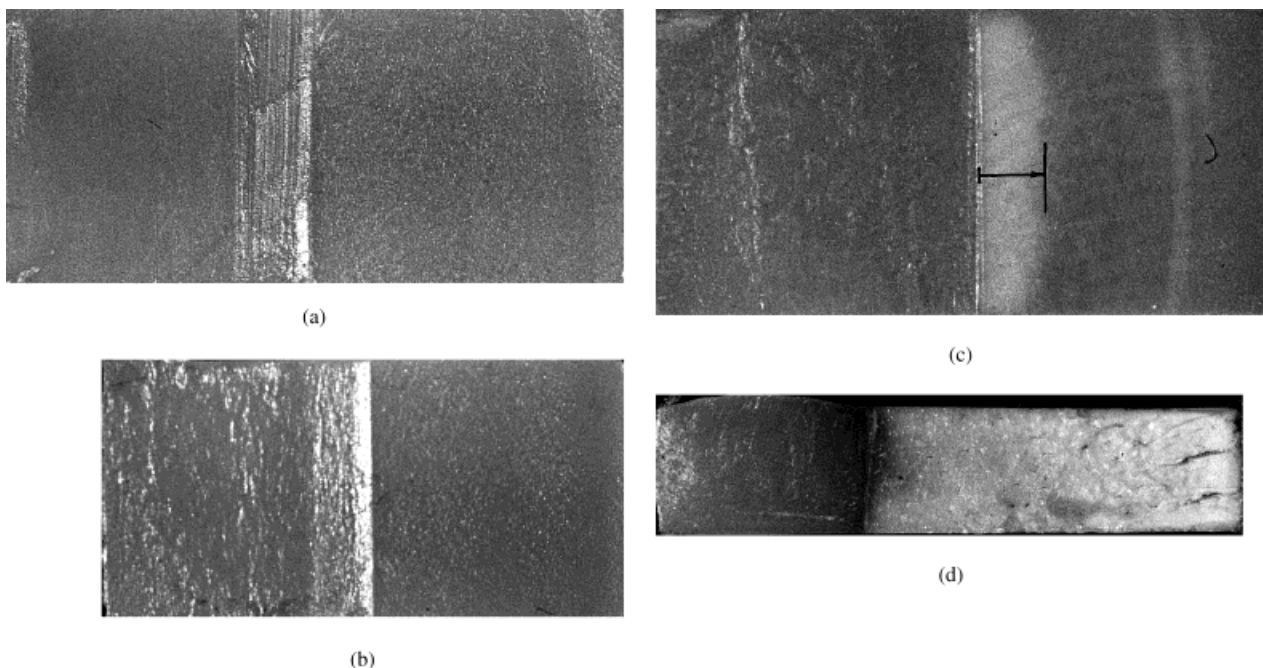


**Figure 6** Fracture surface of propylene samples broken under dynamic loading conditions (direction of propagation from left to right). (a) PPH, (b) PPH-150, (c) PPBC, (d) PPRC.

ance of the fracture surface with the naked eye, by watching if the surface exhibits a whitening effect or not due to voiding and craze formation. Photographs of fracture surfaces are shown in Figure 6.

Both homopolymer samples (PPH, PPH-150) displayed no stress whitening, showing completely brittle fracture in contrast with the behavior displayed under static conditions [Fig. 6(a) and (b)]. The brittle nature of the failure is caused mainly by the high speed of the impact test because in a slow speed notch-bending tests specimens were not notch brittle (see Fracture Static Experiments section).

A sharply defined white halo corresponding to the crazed zone, ahead of the crack tip developed prior to crack advance, is, however, clearly visible in the micrograph corresponding to the PPBC sample [Fig. 6(c)]. Again, the fracture feature was different from the stable crack propagation zone displayed by the static experiments, and somewhat different by the pattern displayed by the homopolymer in which plastic deformation mechanisms were completely suppressed. In the center of the specimen the whitened halo had propagated further ahead than at the edges of the crack front, indicating the more critical three-dimensional stress state generated in the interior of the

material. The length of the plastic zone,  $r_p$ , at the plane strain<sup>44</sup> (in the center of the specimen) was directly measured from the fracture surface and used to correct the initial crack length, as indicated in the photograph [Fig. 6(c)] as explained in the Semibrittle Regime section.

In both cases (homopolymer and block copolymer) the source of brittleness or the inhibition of voiding processes active under static conditions was basically controlled by the high rate, even if some notch sensitivity was detected, as explained in the Conventional Impact Testing section. This provides additional evidence of the importance of impact testing in propylene polymers.

All the broken samples of the PPRC material displayed complete whitening on the fracture surfaces [Fig. 6(d)], indicating that the yielding processes had taken place through the whole resistant section of the specimens assayed. The plastic zone depth penetrated considerably outside the process zone, as can be appreciated from the necked material along the sides of the samples. Thus, the condition of the fully yielded ligament was reached, and hence, the applicability of the Essential work method was, in principle, possible.

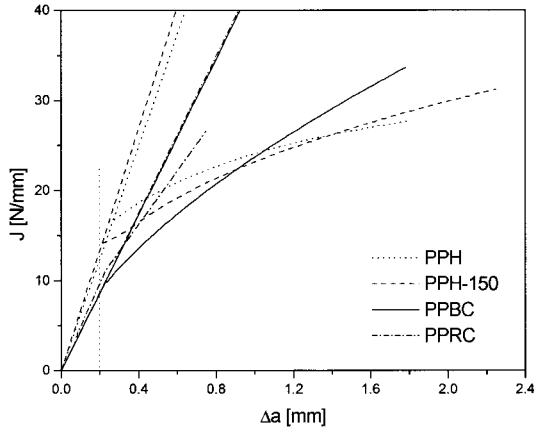


**Figure 7** Integral- $J$  vs. crack extension for the different propylene polymers obtained under static loading conditions.

**Fracture Mechanics Measurements**

Fracture mechanics quantities are expected to be more sensitive than other properties. According to the behavior displayed by each material, the appropriate fracture mechanics procedure was used as explained in the Fracture Mechanics Data Analysis section. The results of data analysis are summarized in Table II, and the corresponding plots are shown in Figures 7 and 8. The good fittings obtained also confirm the conclusions arisen from the qualitative naked-eye analysis carried out on the fracture surface features regarding the nature of the crack propagation regime. Thus, it appears that the model chosen in any case was appropriate. The Normalization  $J$ -method worked very well, and allowed us to easily calculate the  $J$ - $R$  curves of all materials under static loading conditions. Under dynamic conditions different approaches were used, and they were found to be adequate in each case.

The elastic corrected method used in the case of the block copolymer was simple to apply, because  $r_p$  may be easily physically measured from the fracture surface, as explained in the Fractographic section avoiding the need of an iterative process. The size of the plastic zone met the condition of being small compared to the initial crack length and the other in-plane dimensions.

The specific fracture work concept has been successfully applied to characterize the fracture behavior of the random copolymer. Crack growth started after a complete yielded ligament had developed, and thus the energy was mainly expended in propagating the crack through the

specimen.<sup>45</sup> The geometrical condition for the plane strain cannot be exactly calculated because  $\sigma_y$  at crack tip strain rate is unknown, and  $w_e$  should be taken only as a “near plane strain

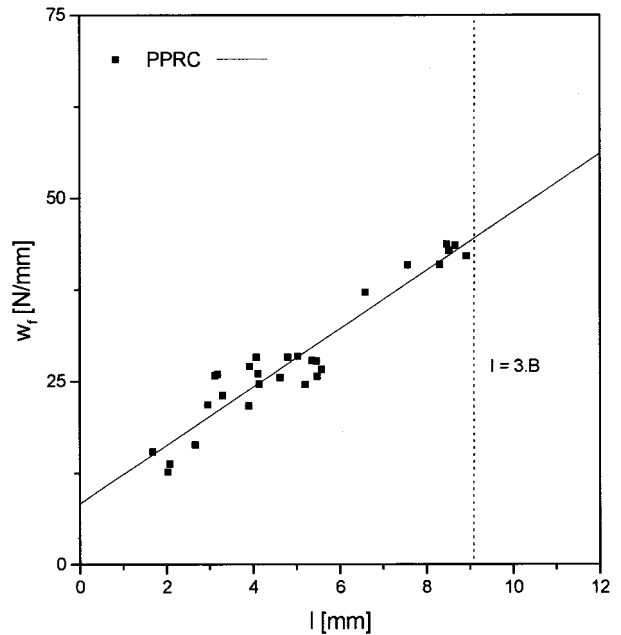
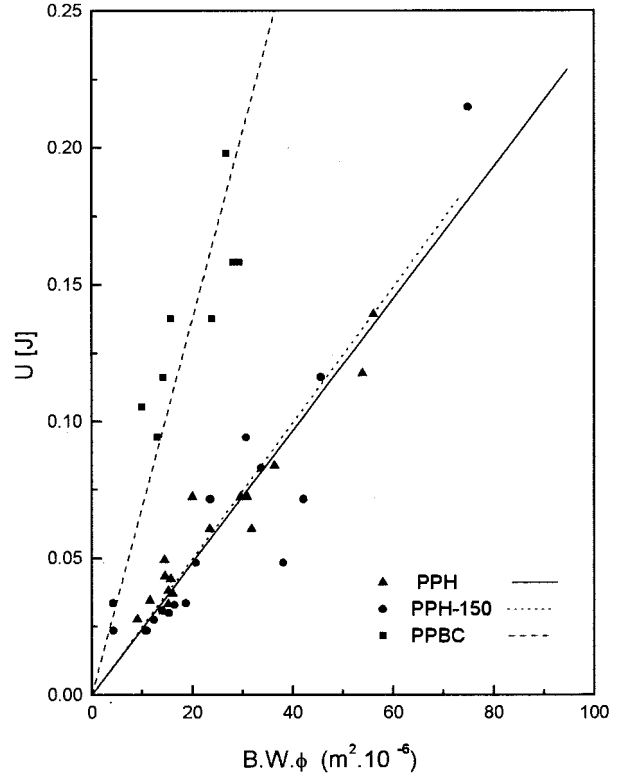


**Figure 8** Dynamic Fracture Mechanics methodologies. (a) Elastic and Corrected Elastic methods, (b) Essential Work of Fracture approach.

value."<sup>46</sup> The resulting parameters are in agree with previous findings<sup>13,47-51</sup> reported for similar polymers.

For plane strain linear elastic behavior  $J_C$  becomes identical to the critical strain energy release rate,  $G_{IC}$ .<sup>52</sup> Mai and Cotterel<sup>46</sup> using geometric similarity arguments between  $J$  and  $w_f$  demonstrated that  $w_e$  is equivalent to  $J_C$ . Therefore, the different parameters can be compared among them.

Large differences in behavior, as explained in the above section, as well as in the critical parameters values, were found under static and dynamic conditions. To summarize the results of the present work, the values of several fracture parameters are shown in Table II.

Under static conditions, even if PPH exhibited the ductile instability in the propagation stage, all materials exhibited very high  $J_{IC}$  values, in agreement with previous measurements in similar materials.<sup>13,49,50,53</sup> The extremely high critical parameter values displayed may simply be interpreted in terms of  $J_C = COD \cdot \sigma_y$ .<sup>28</sup>  $\sigma_y$  may be related to yield phenomena in the process zone and  $COD$  to the deformation process taking place in the highly stressed failure zone at the crack tip.  $COD$  can be considered as a first approximation as proportional to the load point displacement.<sup>54</sup>  $\sigma_y$  is considerably higher for the homopolymers, while the displacement at  $J_{0,2}$  was practically the same for PPH, PPH-150, and PPBC (at about 1.5 mm), while the one corresponding to PPRC was larger (at about 2.5 mm). High  $J_C$  values are related to a combined high  $\sigma_y$  and  $COD$  values.

The tests carried out through this article show Propylene polymers, especially the homopolymer, as very rate-sensitive materials. Both homopolymers displayed practically the same  $G_{IC}$  value, remarkable lower than the ones obtained in the static experiments due to the suppression of microvoiding and crazing at high loading rates. Other polymers such as ABS<sup>28</sup> did not show such large differences between static and impact conditions. It is important to underline the fact that, when applied to impact testing, fracture mechanics (precracked experiments) is able to provide a more detailed description of the mechanical properties of the material than conventional impact tests. In particular, it can be a more selective instrument than, for example, tensile test or the Charpy or Izod strength test, as explained above. In fact, in analyzing the two homopolymers PPH and PPH-150 according to ASTM-D256, it appears that the thermal treatment improves im-

pact performance. However, the Energy Release Rate Critical Parameters are very similar; therefore, the better performance displayed by the annealed homopolymer in Charpy tests may arise from the differences in the initiation processes.

The block copolymer exhibited a very high resistance to crack initiation,<sup>48</sup> evident from higher dynamic toughness values than homopolymers and consistent with the high impact strength. Even if the impact critical parameter was lower than the one obtained at low deformation rates, their values were close.

The better performance under dynamic condition was displayed by the random copolymer.  $w_e$  value was practically the same as the  $J_{0,2}$  determined under static conditions, and fracture still occurred in a stable manner.

## SUMMARY AND CONCLUSIONS

Several commercial-grade propylene polymers (an isotactic homopolymer, a block copolymer, and a random copolymer), exhibiting differences in their mechanical behavior, were mechanically evaluated under static and dynamic conditions.

Stress-strain tensile experiments shows that the homopolymer formed a nonstable neck with localized stress whitening, the 150°C annealed homopolymer, and the block copolymer extended uniformly up to fracture with diffused stress whitening and without necking, while the random copolymer formed a very marked stable neck. The differences in tensile behavior were revealed in the fracture propagation mode displayed by each propylene polymer under dynamic conditions. Static Fracture experiments revealed that all materials exhibited nonlinear load-line displacement behavior under static conditions due to the growth of a significant damage zone at the crack tip. In the case of the nonthermally treated homopolymer a sudden instability occurred after some degree of crack advance while all the other polymers exhibited a stable fracture manner. Hence,  $J$ - $R$  curves were constructed. Both homopolymers displayed the highest initiation values consistent with the highest  $\sigma_y$  values.

However, under dynamics, the stress whitening exhibited under static conditions<sup>54</sup> were totally suppressed for the homopolymer and partially suppressed for the block copolymer; the random copolymer, however, still exhibited clear signs of plastic deformation. According to the behavior displayed by each material and adequate

fracture methodology involving only the determination of total energy to fracture were applied to evaluate critical parameters. Under this condition the ranking of the materials changed and both modified propylene showed up the highest critical values consistent with the development of plasticity.

Some notch sensitivity turned out from the impact tensile, notched, and unnotched Charpy tests. Conventional impact testing appears to be nonselective methods and mainly controlled by initiation processes.

The experiments shown here illustrates that fracture impact testing appears to be very important in assaying this kind of materials. Some propylene polymers that exhibit tough, ductile failures when tested at a low or moderate strain rate may suffer brittle fracture under impact loading when the strain rate is relatively high, because plastic deformation mechanisms are suppressed.

In addition, the specific essential fracture work concept has been successfully applied to characterize the fracture behavior of the random propylene copolymer that fractured after complete fully plastically deformed ligament conditions. This methodology may be considered as a potential useful technique for determining high-rate material toughness in grossly plastic fracture conditions, and very promising as an alternative to that of the *J*-Integral method (*J-R* curve), which implies stopping the experiment from outside. Further work is in progress regarding this latter issue.

The financial support of this work by CONICET (PIP 4394/96) and ANPCYT (14-00000-00303) is gratefully acknowledged.

## REFERENCES

- Karger-Kocsis, J. Polypropylene: Structure and Morphology; Chapman and Hall: London, 1995.
- Karger-Kocsis, J.; Varga, J.; Ehrenstein, G. W. *J Appl Polym Sci* 1997, 64, 2057.
- Varga, J. *J Mater Sci* 2557.
- Williams, J. G. Fracture Mechanics of Polymer; Ellis Horwood Ltd.: London, 1984, p. 237.
- Kinloch, A. J.; Young, R. J. In Fracture Behavior of Polymers; Applied Science Publisher Ltd.; London, 1983, p. 182.
- Savadori, A. *Polym Testing* 1985, 5, 470.
- Plati, E.; Williams, J. G. *Polym Eng Sci* 1975, 15, 470.
- Ivankovic, A.; Williams, J. G. *Int J Fract* 1993, 64, 251.
- Martinatti, F.; Ricco, T. In Proceedings of Impact and Dynamic Fracture of Polymers and Composites; Williams, J. G.; Pavan, A., Eds.; ESIS 19: Mechanical Engineering Publications: London, 1995.
- Coppola, F.; Greco, R.; Ragosta, G. *J Mater Sci* 1986, 23, 1775.
- Newman, L. V.; Williams, J. G. *Polym Eng Sci* 1978, 18, 893.
- Vu-Khanh, T.; De Charentenay, F. X. *Polym Eng Sci* 1985, 25, 841.
- Frontini, P. M.; Fave, A. *J Mater Sci* 1995, 30, 2446.
- Ireland, D. R. Instrumented Impact Testing; ASTM STP563, 1973, p. 412.
- Cernal, C. R.; Cassanelli, A. N.; Frontini, P. M. *Polym Test* 1995, 14, 85.
- Bernal, C. R.; Montemartini, P. E.; Frontini, P. M. *J Polym Sci Part B Phys Ed* 1996, 34, 1869.
- Bernal, C. R.; Frontini, P. M.; Rink, M. *Macromol Symp* 1999, in press.
- Garcia Brosa, V.; Bernal, C.; Frontini, P. *Eng Fract Mech* 1999, 62, 231.
- Landes, J. D.; Zhou, Z. *Int J Fract* 1993, 63, 383.
- Che, M.; Grellmann, W.; Seidler, S.; Landes, J. D. *Fatigue Fract Eng Mater Struct* 1977, 20, 119.
- Zhou, Z.; Landes, J. D.; Huang, D. D. *Polym Eng Sci* 1994, 34, 128.
- European Structural Integrity Society (ESIS), Technical Committee 4, Polymers and Composites, A Testing Protocol for Conduction J-Crack Growth Resistance Curve Tests on Plastics, 1992.
- Williams, J. G. In Fracture Mechanics of Polymers; Ellis Horwood Ltd.: London, 1984, p. 69.
- Williams, J. G. In Fracture Mechanics of Polymers; Ellis Horwood Ltd.: London, 1984, p. 67.
- Hodgkinson, J. M.; Chow, K. H. L.; Williams, J. G. In Proceedings of the 8th International Conference on Deformation Yield and Fracture of Polymers, 43/1 8-11, The Institute of Materials: London, 1991.
- Vu-Khanh, T. *Polymer* 1988, 29, 1979.
- Crouch, B. A.; Huang, D. D. *J Mater Sci* 1994, 29, 861.
- Castellani, L.; Frassine, R.; Pavan, A.; Rink, M. *Polymer* 1996, 37, 1329.
- Chan, W. Y. F.; Williams, J. G. *Polymer*, 1994, 35, 1666.
- Paton, C. A.; Hashemi, S. *J Mater Sci* 1992, 27, 2279.
- Mai, Y.-W.; Powell, P. *J Polym Sci Part B Polym Phys* 1991, 29, 785.
- Hashemi, S. *J Mater Sci* 1993, 28 6178.
- Hashemi, S.; O'Brien, D. *J Mater Sci* 1993, 28, 3977.
- Pegoretti, A.; Marchi, A.; Ricco, T. *Polym Eng Sci* 1997, 37, 1047.
- Yap, O. F.; Mai, Y. W.; Cotterell, B. *J Mater Sci* 1983, 18, 657.

36. Karger-Kocsis, J.; Czigány, T; Moskala, E. *Polymer* 1977, 38, 4587.
37. Mai, Y.-W.; Cotterell, B. *Int J Fract* 1986, 32, 105.
38. Mai, Y.-W.; Powel, P. *J Polym Sci Part B Polym Phys* 1991, 29, 791.
39. Salemi, A. S.; Nairn, J. A. *Polym Eng Sci* 1991, 30, 211.
40. Kinloch, A. J.; Young, R. J. In *Fracture Behaviour of Polymers*; Applied Science Publishers Ltd.: London, 1983, p. 189.
41. Vu-Khanh, T.; Sancharuin, B.; Fisa, B *Polym Compos* 1985, 6, 249.
42. Vu-Khanh, T.; Fisa, B. *Theoret Appl Fract Mech* 1990, 13, 11.
43. Narisawa, I. *Polym Eng Sci* 1987, 27, 41.
44. Moskala, R. P. E. J. *J Mater Sci* 1992, 27, 4883.
45. Mai, Y.-W. *Int J Fract* 1993, 35, 995.
46. Mai, Y.-W.; Cotterell, B. *Int J Fract* 1986, 32, 105.
47. Hodgkinson, J. M.; Savadori, A.; williams, J. G. *J Mater Sci* 1983, 18, 2319.
48. Bramuzzo, M. *Polym Eng Sci* 1989, 29, 1077.
49. Fernando, P. L.; Williams, J. G. *Polym Eng Sci* 1980, 20, 215.
50. Frenando, P. L.; Williams, J. G. *Polym Eng Sci* 1981, 21, 1019.
51. Carpinteri, A.; Marega, C.; Savadori, A. *J Mater Sci* 1986, 21, 4173.
52. Xavier, S. F.; Schutz, J. M.; Friedrich, K. *J Mater Sci* 1990, 25, 2411.
53. Williams, J. G. In *Fracture Mechanics of Polymers*; Ellis Horwood Ltd.: London, 1984, p. 157.
54. Fernando, P. L.; Williams, J. G. *Polym Eng Sci* 1981, 21, 1003.